SNOWFALL MEASUREMENTS BY PROPOSED EUROPEAN GPM MISSION

Alberto Mugnai [1], Sabatino Di Michele [1], Eric A. Smith [2], Fabrizio Baordo [1], Peter Bauer [3], Bizzarro Bizzarri [1], Paul Joe [4], Christopher Kidd [5], Frank S. Marzano [6], Alessandra Tassa [1], Jacques Testud [7], and Gregory J. Tripoli [8]

[1] *Istituto di Scienze dell'Atmosfera e del Clima, Consiglio Nazionale delle Ricerche, Roma, ITALY*
[2] *Goddard Space Flight Center, National Aeronautics and Space Administration, Greenbelt, MD, USA*
[3] *European Centre for Medium-range Weather Forecasts, Shinfield Park, Reading, UK*
[4] *Meteorological Service of Canada, Downsview, Ontario, CANADA*
[5] *School of Geography, Earth and Environmental Sciences, Univ. of Birmingham, Edgbaston Birmingham, UK*
[6] *Dipartimento di Ingegneria Elettrica, Università dell'Aquila, L'Aquila, ITALY*
[7] *Novel Initiative for Meteorological and Environment Technologies (NOVIMET), Vélizy, FRANCE*
[8] *Department of Atmospheric and Oceanic Sciences, University of Wisconsin, Madison, WI, USA*

Abstract: The European Space Agency (ESA) is currently engaged in a Phase A study of the European Global Precipitation Measurement (EGPM) Mission. This represents both a dedicated ESA mission primarily supporting research and applications in the European Community and Canada, and a contributed spacecraft element and scientific research component for the International GPM Constellation Mission. The scientific payload of the EGPM satellite consists of a multispectral, conically-scanning microwave radiometer and a 3-beam, nadir-pointing Ka-band rain radar. The radiometer operates at four window frequencies from cm to mm wavelengths (18.7, 36.5, 89.0, and 150.0 GHz), at one water vapor absorption frequency on the far wing of the 22.235 GHz H_2O line (23.8 GHz), at four temperature sounding frequencies within 50-54 GHz on the low frequency wing of the 60 GHz molecular Oxygen complex, and at four complimentary-paired sounding frequencies in the vicinity of the strong 118.75 O_2 line. The EGPM measurements will make contributions to a number of important scientific topics vis-à-vis precipitation science and the Earth's climatically varying water cycle. In this investigation, we examine the specific contribution of the EGPM satellite to snowfall measurement. This is achieved by synthetically calculating both the radiative observations generated by the EGPM radar - radiometer instrument suite and the consequent precipitation estimates for a numerically simulated snowstorm. The storm simulation is performed by means of a time - dependent, 3-dimensional, cloud / mesoscale model using explicit multi-species microphysics. The results demonstrate that because of its unprecedented sensor / channel capacity, the EGPM mission is expected to make significant improvements in the measurement of snowfall, to extend the observed precipitation spectrum as retrieved from space, and ultimately to improve the understanding and closure of the global water cycle.

1. INTRODUCTION

The Earth has a yearly precipitation average of some 690 mm of which about 5% is produced in the form of snowfall. There is a strong latitudinal influence in which the snowfall proportion increases dramatically as a function of latitude, particularly light snowfall, while the total precipitation amounts undergo steady decreases from the relative maxima positioned at the average latitudes of the northern and southern hemisphere midlatitude storm tracks (~40ºN / 45ºS). As a consequence, in the central and northern regions of Europe, North America, and Asia, since snowfall represents a significant portion of the total precipitation amount, it becomes the main driver of the regional water cycle process, whose influence extends to the entire globe. For instance, while the typical annual average precipitation total in Canada is 535 mm, with 36% falling as snow, in northern Canada the proportion of snowfall to total precipitation ramps up to approximately 90%, almost all of which is produced in the form light snowfall. Therefore, light snowfall, and a smaller component of light rainfall, are key drivers to water cycling in mid to northern latitudes. This issue is manifest in seeking to understand how snow accumulation is changing in the context of the current global warming epoch (e.g., see Zwally 1989).

These elements of precipitation are brought out in the latitude - precipitation rate category diagram shown in Figure 1a, a diagram produced from the Comprehensive Ocean - Atmosphere Data Set (COADS). [COADS is a climatology of oceanic meteorological and sea surface observations recorded on ships; see da Silva et al. (1994).] The figure illustrates the latitudinal distribution of cumulative percentage of light snowfall occurrence (indicated in gray as frozen precipitation) and light rain occurrence (indicated in blue as liquid precipitation), as given by the COADS climatology. Note the white region above the colored region of the diagram indicates the cumulative remainder of moderate to heavy rain occurrences, where 1 mm hr^{-1} is taken as the approximate threshold between light and moderate rain rate. Also, note there are minor contributions by mixed phase precipitation at the ocean surface. It is immediately evident from this figure how important light rainfall and snowfall, particularly light snowfall, are to the water budget poleward of the 30 degree parallels. Figure 1b provides a further illustration of the relevance of light rainfall and snowfall to the water budget poleward of ~45ºN in the northern hemisphere. In the upper-left panel of this figure, there is a comparison of rain rates between Europe and the Tropics which emphasizes the great disparity between rain rate intensities between these two regions of the globe. In the upper-right panel, there is a set of cumulative distribution functions (CDFs), given in terms of snow water equivalent rate, at four measurement locations from mid to northern latitudes -- showing that at least 90% of the precipitation occurs at rates less than 3 mm hr^{-1}. Finally, in the lower-left panel, there are a set of three graphs indicating snow to total precipitation ratios at three locations situated between 45ºN to 82ºN in Canada, indicating that in moving from the southern-most point to the northern-most point, snowfall fractions rise from ~30% to ~90%.

In examining these two figures, it should be recognized that the core satellite of the GPM mission, which will also fly an advanced radar - radiometer payload (i.e., a dual-frequency Ku / Ka-band radar and a hi-resolution conically-scanning radiometer), will only reach the ±65 degree parallels given its anticipated orbit inclination of 65 degrees. Therefore, all measuring of the high-latitude water budget will become the realm of the EGPM mission. Moreover, all measurement of light rainfall and snowfall producing radar reflectivity factor signatures below ~12 dBZ (i.e., sensitivity of the GPM core satellite's Ka-band radar), must be done by the EGPM radar whose sensitivity will be considerably higher (~5 dBZ).

Detailed knowledge of the spatial distribution of snowfall is vital for a number of scientific applications. Additionally, since climate models suggest that climate change will be a first most evident in polar regions, monitoring snowfall may provide the optimal means to test the hydrological component of the models. However, snowfall measurements are difficult to make due to strong wind effects on snow gauges -- especially for light snowfall, which drifts, blows away, evaporates, and melts, often before it can be measured. In addition, ground-based measurement sites are sparse in remote or mountainous regions, thus resulting in poor knowledge of snowfall at such locations. Therefore, satellites are the only

viable means for providing areally extended snowfall measurements -- although current satellite sensor systems have not been specifically designed to measure snowfall accumulation or snowfall rate.

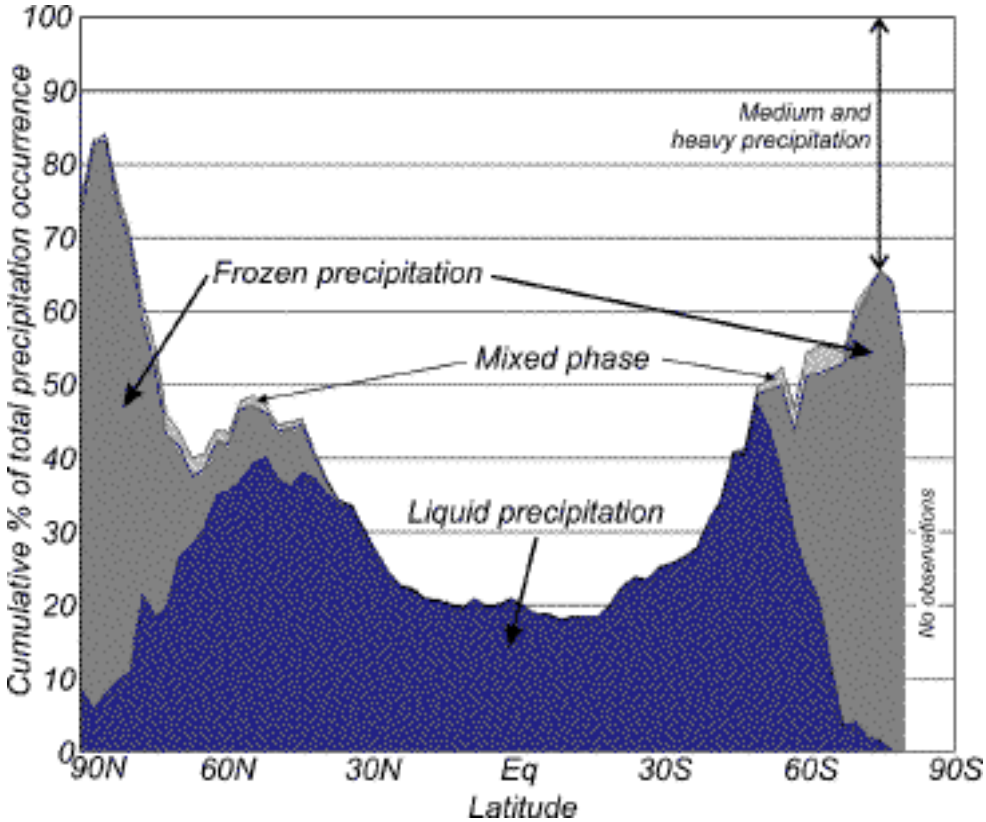

Figure 1a: Latitude - precipitation rate category diagram as derived from COADS dataset. [See text for explanation.]

In principle, such measurements can be made by space-borne microwave radiometers employing frequencies above 30 GHz that respond to scattering by ice particles. However, highly variable radiation emission by the underlying land surface generally obfuscates retrieval of snowfall based on measurements at microwave window frequencies (i.e., frequencies for which the atmosphere is relatively transparent with respect to the neighboring spectrum). That is why Special Sensor Microwave/Imager (SSM/I) radiometers and multichannel precursor radiometers that began operating in 1978 at window frequencies up to 85 GHz (Kramer, 2002) have not been used successfully to measure snowfall from space.

This problem has been partially overcome with the launch in 1998 of the first of the 5th generation of operational polar orbiting satellites of the U.S. National Oceanic and Atmospheric Administration (i.e., NOAA-15). This platform carries the Advanced Microwave Sounding Unit (AMSU) – see Kramer (2002) for details. AMSU is a 20-channel microwave radiometer, comprised of three separate cross-scanning units: AMSU-A1, AMSU-A2 and AMSU-B. AMSU-A1 has 12 channels in the 50-60 GHz molecular oxygen band for atmospheric temperature profiling, while AMSU-B has two high-frequency window channels at 89 and 150 GHz and three split-band channels (183.31±1, 183.31±3, 183.31±7 GHz) surrounding the strong water vapor line at 183.31 GHz for atmospheric humidity profiling. These channels are sensitive to scattering by precipitating snow, and since they permit partial to full obscuration of emission from the underlying land surface, they can be used to retrieve snowfall within the atmosphere. Empirical relationships to detect snowfall from AMSU measurements have been recently published by

Kongoli et al. (2003), while Skofronick-Jackson et al. (2004) are using a physical approach to retrieve snowfall over land from AMSU-B measurements.

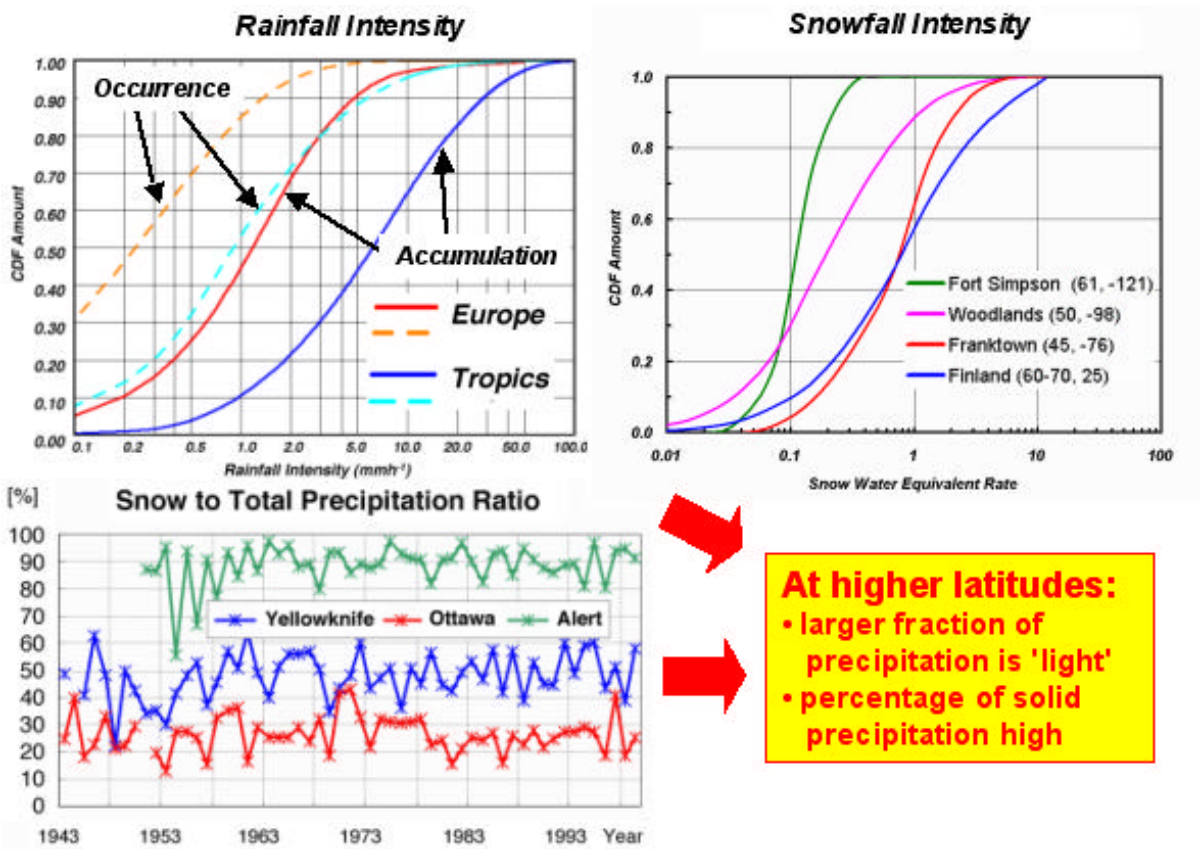

Figure 1b*:* Upper-left panel indicates differences in properties of rainfall intensity (abscissa) between Europe and Tropics in terms of CDFs of accumulation and occurrence. Upper-right panel indicates CDFs as function of snow water equivalent rate (mm hr^{-1}) for four locations in mid to northern latitudes: (1) Fort Simpson, NW Territories, (2) Woodlands, Manitoba, (3) Franktown, Ontario, and nation of Finland (latitude-longitude coordinates given in parentheses). Lower left panel indicates snow to total precipitation ratio (in percent) for three different locations: (1) Ottawa, Ontario at ~45ºN, (2) Yellow Knife, NW Territories at ~62ºN, and (3) Alert, Ellesmere Island (NW Territories) at ~82ºN.

Snowfall detection and measurement is a main driving requirement of the EGPM mission, now in progress of a Phase A study by the European Space Agency (ESA). The EGPM mission has been proposed by a precipitation / water budget-focused international scientific community, primarily from Europe and Canada, but also including scientists from the U.S. and Japan. The main scientific objectives of the EGPM mission are centric to current research problems in Europe and Canada, but the mission also has been proposed as a participant in the International Global Precipitation Measurement (GPM) Mission as a dedicated member of the GPM constellation. The article by see Smith et al. (2004) in this same volume describes the International GPM Mission. The EGPM mission is specifically designed to detect and measure snowfall, light rain, and warm rain -- both over land and ocean -- particularly in mid and northern latitude climates. That is what the mission requires an advanced and unprecedented scientific payload. The payload consists of: (1) an innovative conically scanning microwave radiometer combining the conventional rain-measuring window channels of 18, 23, 37, and 85 GHz, a high-frequency window

channel at 150 GHz, and four cross-paired temperature-sounding channels near 52 and 118 GHz (four channels in each O_2 absorption region); and (2) a Ka-band (35.6 GHz) 3-beam nadir-pointing precipitation radar having a sensitivity of ~5 dBZ.

The sounding channels respond to scattering by snow and are less sensitive to surface emission than the window channels. Additionally, coupled radiometric observations within the strong oxygen absorption band between 50-54 GHz and near the strong O_2 absorption line at 118.75 GHz, permit the accurate retrieval of precipitation information by exploiting differential atmospheric absorption within each band and differential hydrometeor scattering between the two bands. Choosing pairs of frequencies in the two O_2 absorption regions that have similar weighting functions for clear skies over precipitating clouds, enables vertical partitioning (slicing) of the frozen cloud constituents. This partitioning results from a combination of: (a) differences in cross-frequency band upwelling brightness temperatures (T_Bs) originating from large hydrometeor scattering (with higher frequency T_Bs appearing colder than lower frequency T_Bs -- i.e., differential scattering), and (b) differences in within-frequency band upwelling T_Bs originating from molecular oxygen emission (with far-wing T_Bs providing greater cloud depth penetration than near-wing T_Bs -- i.e., differential absorption). In essence, a sequence of corresponding channel pairs provides profile information on snow amount from cloud top to monotonically increasing depths inside the cloud (depth being defined from the top-down perspective). It is important to recognize that the AMSU instrument does not have similar snow measuring potential because it lacks any type of coupling between its oxygen band and water vapor line sounding channels.

The potential of this approach was first investigated by Gasiewski and Staelin (1990). Lately, Blackwell et al. (2001) performed an analysis of the observations that were taken in these two oxygen bands by the airborne NPOESS Aircraft Sounder Testbed-Microwave (NAST-M) instrument during the Convection and Moisture Experiment (CAMEX-3) campaign in Summer 1998. This instrument consists of two radiometers, one with 8 channels covering the 50-57 GHz portion of the oxygen complex (the so-called 54-GHz radiometer), and the other with 9 split band (double-sideband) channels around the 118.75 oxygen line (the so-called 118-GHz radiometer). More recently, Bauer and Mugnai (2003) used NAST-M observations of hurricane Bonnie to demonstrate the potential of these temperature-sounding channels for precipitation profile retrieval from space.

Based on the above noted analyses, four pairs of sounding channels are proposed for the EGPM radiometer. The lower four channels match the NAST-M 54-GHz radiometer (53.75, 52.8, 51.76, and 50.30 GHz), these channels enabling ever-increasing penetration depths into a precipitating cloud. The corresponding channels near 118.75 GHz are 118.75±8.5, 118.75±4.2, 118.75±2.3, and 118.75±1.2 GHz, respectively. These are determined by matching their clear-sky weighting functions with the four corresponding 50-54 GHz channels based on calculations with some 55,000 atmospheric profiles.

In the following analysis, we examine the performance of the EGPM scientific payload (radar + radiometer) for snowfall measuring, by estimating with a radiative transfer model, the relevant radiometer and radar observations and respective precipitation retrievals associated with a major snowstorm over the eastern United States. The storm is initially simulated by means of a time-dependent, 3-dimensional mesoscale model run in cloud-resolving model mode (CRM-mode) with explicit 2-water / 4-ice microphysics.

2. SIMULATION OF U.S. EAST COAST SNOWSTORM

We use a numerical simulation of a meteorologically prominent snowstorm which occurred over the U.S. east coast during 24-26 January 2000. The simulation was produced by the University of Wisconsin Nonhydrostatic Modeling System (UW-NMS), a 3-dimensional, time-dependent mesoscale model, run in CRM mode with explicit / 6-species microphysics. The six species consist of suspended liquid and frozen cloud hydrometeors (cloud drops and pristine ice crystals), precipitating rain drops, and three forms of

precipitating ice particles (snowflakes, aggregates, and graupel-hail). A detailed description of the original model is found in Tripoli (1992). The simulation was run for a 53.5-hour period from 00:00 UTC January 24 through 05:30 UTC January 26, initialized over the outer grid with ECMWF global analysis information configured within a 2.5-degree mesh. A 3-nest grid system was used with an outer grid resolution of 37.5 km, a transition mesh of 9.38 km grid resolution, and an inner, fine mesh grid resolution of 2.34 km. The inner domain covers a horizontal area of 468 x 468 km^2, extending 17 km in the vertical -- resolved to 39 levels with a height-dependent spacing using highest resolution at lowest levels. Over the first 12 hours of the simulation, only the outer nest was invoked; the second nest was added at 12 hours while the third was inserted at 24 hours. The UW-NMS microphysics scheme was used for each of the three grids, predicting the mixing ratios of the six different hydrometeor species. The medium and inner grids were positioned in such a way to best capture the snow fields, being guided to move northward so as to follow the location of minimum pressure. Figure 2 provides a schematic illustration of the grid nest design.

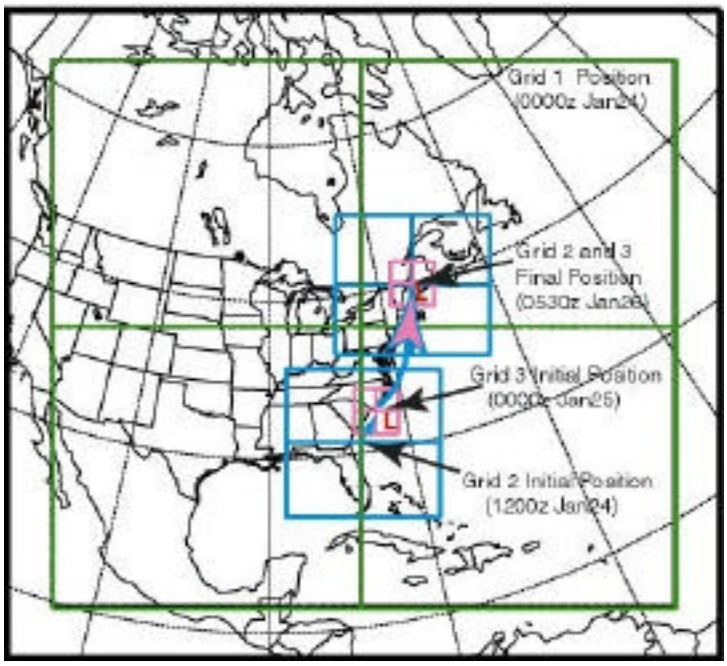

Figure 2: Nested grid system used to perform UW-NMS simulation of 24-26 January 2000 snowstorm over U.S. east coast.

For the analysis, we use model outputs from the inner grid at 06:00 UTC of January 25, 2000. Figure 3 illustrates columnar equivalent water content (CWC) for the six hydrometeor species at this time step. It is evident that heavy rainfall is localized in the top-right (north-eastern) portion of the domain (over warm ocean), with heavy snow present across an extended inland region (over cold terrain).

3. MICROWAVE RADIATIVE TRANSFER MODELING

In order to simulate the upwelling T_Bs that would be observed by the EGPM radiometer, we apply a 3D-adjusted plane-parallel radiative transfer (RTE) model to the microphysical outputs of the simulated snowstorm. The RTE model as been described in the studies of Roberti et al. (1994), Liu et al. (1996), Bauer et al. (1998), and Tassa et al. (2003). For most applications, RTE model-generated upwelling T_Bs over simulated satellite footprints would be calculated at the model resolution (generally higher than the radiometer resolution) and at the radiometer's incident viewing angle (for EGPM this is 53°). The T_Bs

would then be spatially filtered in order to reconcile with the radiometer's effective resolutions for different channels. However, in this sensitivity study, we use upwelling T_Bs at nadir (0° incidence) and at model resolution (2.34 km) since they are more suitable to understand and evaluate the behavior of the different frequencies.

The required inputs to the RTE model are suitable temperature / moisture profiles and temperature / emissivity of the surface, as well as vertical profiles of liquid / ice water contents (LWCs / IWCs) of the various hydrometeors -- along with their single-scattering properties. Surface temperature and vertical profiles are provided by the UW-NMS simulation. Absorption by atmospheric gases at microwave frequencies are calculated according to the Liebe and Gimmestad (1978) and Liebe (1985) clear-moist air refractivity model that provides a combined water vapor – oxygen volume absorption coefficient.

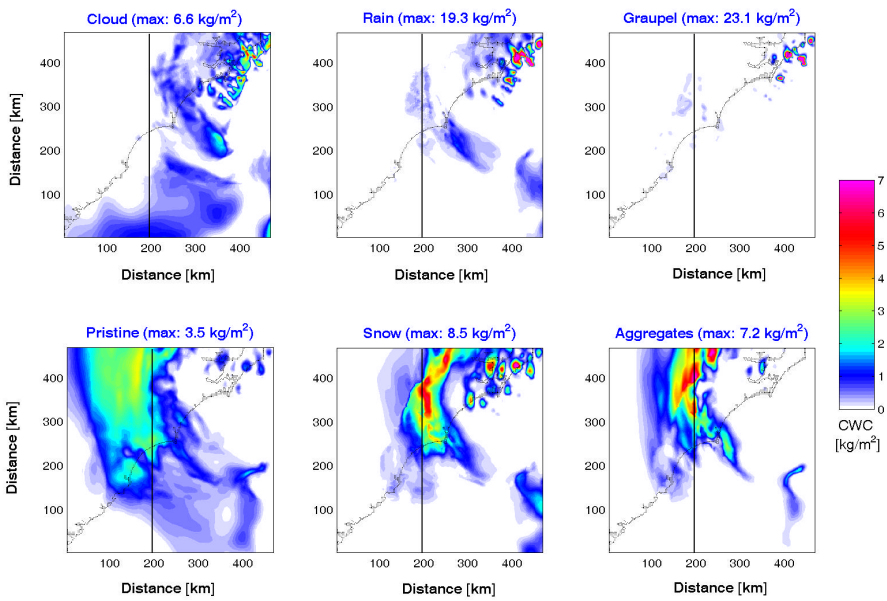

Figure 3: CWCs of six hydrometeor species [cloud droplets (top-left), rain drops (top-middle), graupel (top-right), pristine crystals (bottom-left), snowflakes (bottom-middle), and aggregates (bottom-right)] for inner grid of UW-NMS snowstorm simulation at time step 1800 s (i.e., 06:00 UTC, 25 January 2000). Vertical lines indicate path of vertical cross-section given special attention in latter sections of the paper.

Surface emissivity is assigned dependent upon frequency and surface characteristics (land / ocean, surface roughness, type of soil and soil cover, soil humidity, etc.). While it can be highly variable depending on these parameters, for this study we assume constant values of 0.9 and 0.65 for land and ocean backgrounds, respectively – see Hewison and English (2000) for the emissivity of many land surfaces. The uncertainty in surface emissivity is taken into account within the Bayesian retrieval scheme developed by Mugnai et al. (2001) and Di Michele et al. (2003). This is accomplished by means of an error covariance matrix (see Di Michele et al. 2004), which accounts for T_B sensitivity to parameter uncertainties and approximations used in the forward RTE model (e.g., Tassa et al. 2003, 2004).

Finally, there is a need to determine the single-scattering properties of the various hydrometeor species. This is a straightforward calculation in Mie scattering if only pure water and ice spheres are considered, but can be a major challenge due to the wide variety of sizes, densities, and shapes of natural ice hydrometeors -- especially for snowflakes and ice aggregates which are hydrometeors large enough to interact with the radiometer frequencies of interest, but whose shapes are typically in radical departure

from spheres. However, whereas the UW-NMS model provides hydrometeor size distributions and densities, information on shape is not available from its microphysical parameterization scheme -- which is designed strictly to exchange H_2O mass between vapor and the different species of hydrometeors (under the allowed gas-hydrometeor or hydrometeor-hydrometeor mass transfer schemes) without considering the habits under which the mass transfers take place. For this reason, we take the customary assumption that all particles are spherical and homogeneous so that Mie theory can be applied (Bohren and Huffman, 1983; Wiscombe, 1980).

Graupel particles are assumed to be spherical with densities nearly that of pure ice (i.e., ~0.92 g cm^{-1}). They are assumed to be "equivalent homogeneous spheres" having an effective dielectric function obtained by combining the dielectric functions of ice and air (or water, in case of melting) according to the effective medium Maxwell-Garnett mixing theory for a two-component mixture of inclusions of air (water) in an ice matrix; see Bohren and Huffman (1983). On the other hand, snowflakes and aggregates are low-density, fluffy ice particles (as long as they are completely frozen). As a result, they should not be modeled according to Maxwell-Garnett mixing theory. This is especially the case for equivalent soft-ice spheres having very large asymmetry factors (> 0.9). In essence, the application Maxwell-Garnett theory to assumed "equivalent homogeneous spheres" at the higher microwave frequencies does not adequately "cool" the upwelling radiation.

This problem has been addressed by Skofronick-Jackson et al. (2004) in their attempt to retrieve snowfall over land from AMSU-B measurements, using a physically based retrieval algorithm relying on a CRM simulation of a winter storm. Noteworthy, these authors were able to simulate T_Bs that match the AMSU-B observations, and to obtain retrieved snow masses that are consistent with available radar measurements. They did so by extending the procedure of Grenfell and Warren (1999) to AMSU-B frequencies. They show that the single-scattering properties of nonspherical ice particles across the ultraviolet, optical, and infrared portions of the electromagnetic spectrum are well approximated by a collection of solid ice spheres having the same volume-to-surface-area ratios as nonspherical particles (see also Neshyba et al. 2003). Note that due to mass conservation, each nonspherical particle is represented not by just one sphere, but rather by a number (n) of equal size spheres.

Based on these results, we represent each pristine ice crystal, snowflake, or aggregate particle with an ensemble of equivalent solid ice spheres, all having a diameter determined by the volume to cross-sectional area ratio (V/A) of the original nonspherical ice particle. The volume (V) is provided by the UW-NMS simulation. For calculating cross-sectional area (A), we use the observational relationship $A / (\pi D^2/4) = C_0 * D^C$ that has been published by Heymsfield and Miloshevich (2003) for several different individual particle habits. [Here, D (in cm) is the maximum diameter of the particle and the coefficients C_0 and C (in appropriate cgs units) depend on ice particle habit.] For pristine ice crystals and aggregates, we use values C_0 = 0.18 and C = -0.2707 (indicated by the same authors) as appropriate averages for midlatitude, continental mixed-habit cirrus clouds. For snowflakes, we use values C_0 = 0.6 and C = 0., which are consistent with those given in the same paper for several snow habits. As a result, the diameter (D_s) and the number (n_s) of the equivalent solid-ice spheres are given by:

$$D_s = \frac{\rho}{\rho_{ice}} \frac{D}{C_0 D^C}$$

$$n_s = \frac{C_0}{1-C} \frac{D^{3+C}}{D_s^{\,3}}$$

where a given density ρ of each of three ice categories (i.e., pristine ice crystal, snowflake, aggregate) is given by the UW-NMS model -- and ρ_{ice} = 0.916 g cm^{-3}.

To estimate reflectivities that would be measured by the EGPM 35.6 GHz radar, all ice particles can been modeled by use of Maxwell-Garnett mixing theory which is found to be adequate at this frequency according to Meneghini and Liao (2000).

4. SIMULATED EGPM OBSERVATIONS

To demonstrate the main features that would be observed by the EGPM payload instruments, we now focus on a vertical cross section along the most intense portion of the snowstorm (as is given in Fig. 3). This region is contains frozen precipitation over land. To better understand the relationships between the upwelling T_Bs that would be measured by the EGPM radiometer and the microphysical structure of the simulated storm, we illustrate in Figure 4 the simulated T_Bs together with the columnar water contents for snowflakes and aggregates -- and the vertical profiles of ice water content of total snow along the selected cross section. These results highlight the potential of the various radiometer frequencies for the retrieval of precipitating snow over land. Specifically:

- While the two *lower window frequencies* (18.7 and 23.8 GHz) show little sensitivity to precipitating snowfall over land, significant T_B-depressions (more than 10ºC) are evident at 36.5 GHz in correspondence to the wide portion of the storm (between ~260-390 km along the cross-section), a region characterized by intense snowfall.

- The *higher window frequencies* (89 and 150 GHz) respond very strongly to scattering by snow over land. T_B-depressions up to some 80ºC are observed in correspondence to the deepest snow layer between 340-390 km along the cross-section. The fact that the 89 GHz T_Bs are significantly lower (up to about 40ºC) than those at 150 GHz between 250-320 km, can only be explained by the presence of super-cooled water and small ice particles which reduce the scattering efficiency at 150 GHz more than at 89 GHz. Note that between about 280-300 km, the 89 GHz T_Bs are warmed considerably (up to about 30ºC) by the concurrent presence of a shallow layer of rain mixed with precipitating snow.

- Overall, the *lower frequency* (50-54 GHz) and *higher frequency* (118 GHz) *sounding channels* exhibit similar behavior. They show T_B-depressions due to scattering by snow that increase with snow layer penetration depth – a feature less evident at 53.75 GHz and at 118.75±1.2 GHz because their weighting functions peak above the snow layers. In addition, the various channel pairs exhibit a similar response to rain / snow mixing between ~280-300 km. Nevertheless, the magnitudes of the T_B-depressions are much larger for the higher frequency channels due to the increase in scattering efficiency with frequency. They are as large as 20ºC and 80ºC for the 50-54 GHz band and the 118 GHz line, respectively, in correspondence to the deepest snow layer.

To evaluate the performance of the EGPM radar, we illustrate in Figure 5 the simulated attenuated radar reflectivity at 35.6 GHz for the same snowstorm cross-section of Figure 4. The three dotted lines represent the limits of detection for 0, 5, and 16 dBZ. These results demonstrate that setting a requirement for the EGPM radar sensitivity of ~5 dBZ is very important for the observation of solid precipitation. There is a significant benefit in using this sensitivity limit, rather than something along the lines of the 17 dBZ sensitivity limit used for the Precipitation Radar (PR) onboard the Tropical Rainfall Measuring Mission (TRMM) satellite. As noted in Kramer (2002), the higher sensitivity threshold allows for the detection of light precipitation (which is found at <100 km along the cross-section) and precipitating aggregates (found at >380 km). In addition, with a sensitivity limit of ~5 dBZ, about 1 km of the topmost cloud layer will be detected, a cloud region that will nearly always interact with passive microwave radiometer observations at the higher frequencies. Moreover, there is little to gain in extending the radar sensitivity beyond 5 dBZ -- as clearly illustrated in Figures 6a-b.

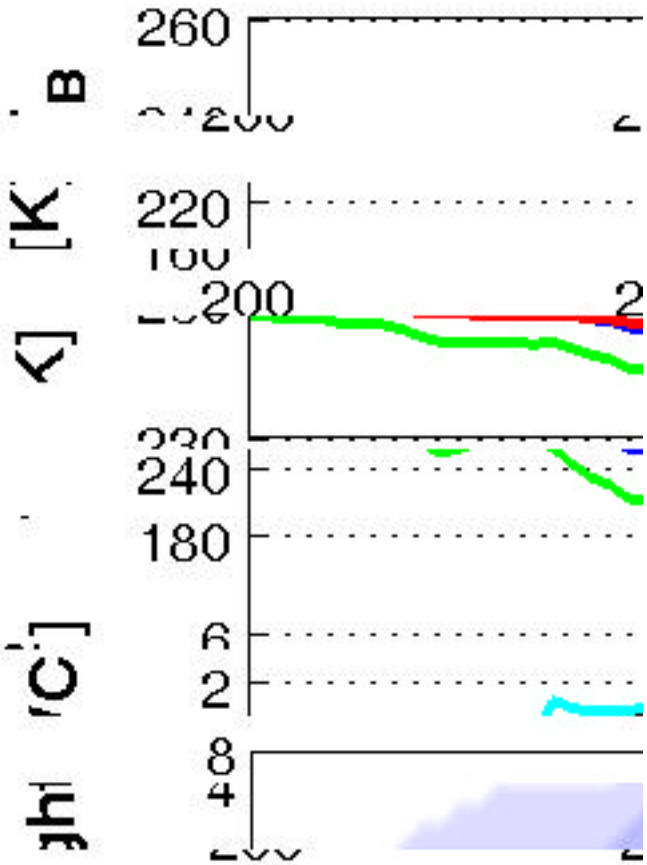

Figure 4: Simulated EGPM radiometer observations for the Eastern US snowstorm (over land). From top to bottom, individual panels show brightness temperatures (T_Bs) at: (1) lower frequency window channels, (2) higher frequency window channels, (3) lower frequency sounding channels, and (4) higher frequency sounding channels -- plus (5) CWCs of key hydrometeors (snowflakes and ice aggregates) and (6) vertical cross-sections of snow IWC.

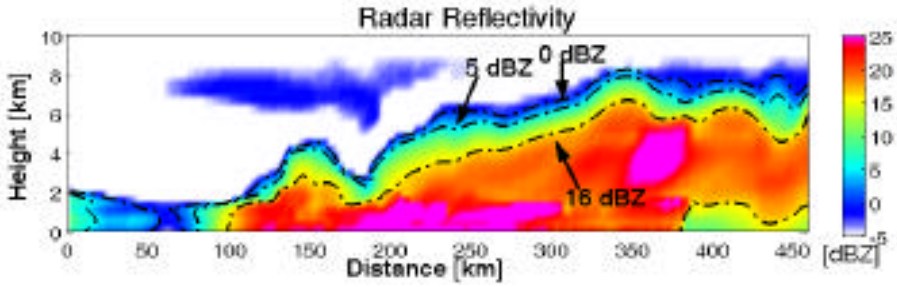

Figure 5*:* Simulated radar reflectivity at 35.6 GHz for selected cross-section of eastern U.S. snowstorm simulation. Dotted lines correspond to three different limits of radar detection sensitivity, specifically 0, 5, and 16 dBZ.

5. SIMULATED EGPM RETRIEVALS

To highlight the improvement in snowfall measurement from space that would be obtained by the EGPM mission, a series of synthetic retrievals have been performed using a snow profiling algorithm (Di Michele et al. 2003) for different combinations of the EGPM radiometer channels, as well as for the EGPM radar-radiometer payload. Results for the selected cross-section of the snowstorm simulation are shown in Figure 7, while Table 1 summarizes the average retrieval accuracy of the near-ground snow IWC for the four different retrievals illustrated in the Fig. 7 panels.

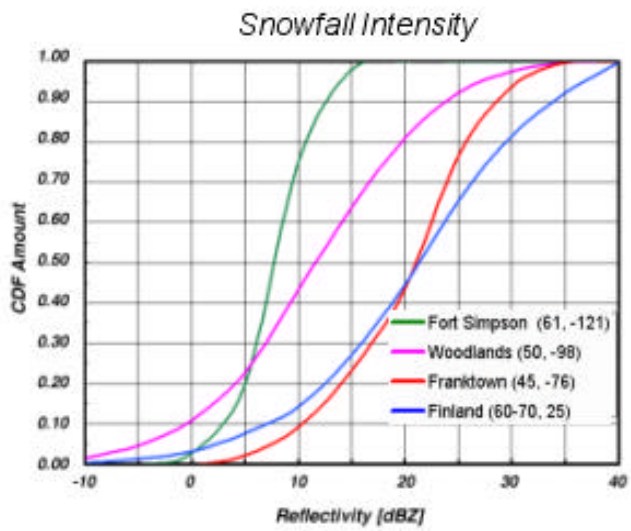

Figure 6a*:* Same as upper-right panel of Fig. 1b, except abscissa is given in term of radar reflectivity factor (dBZ).

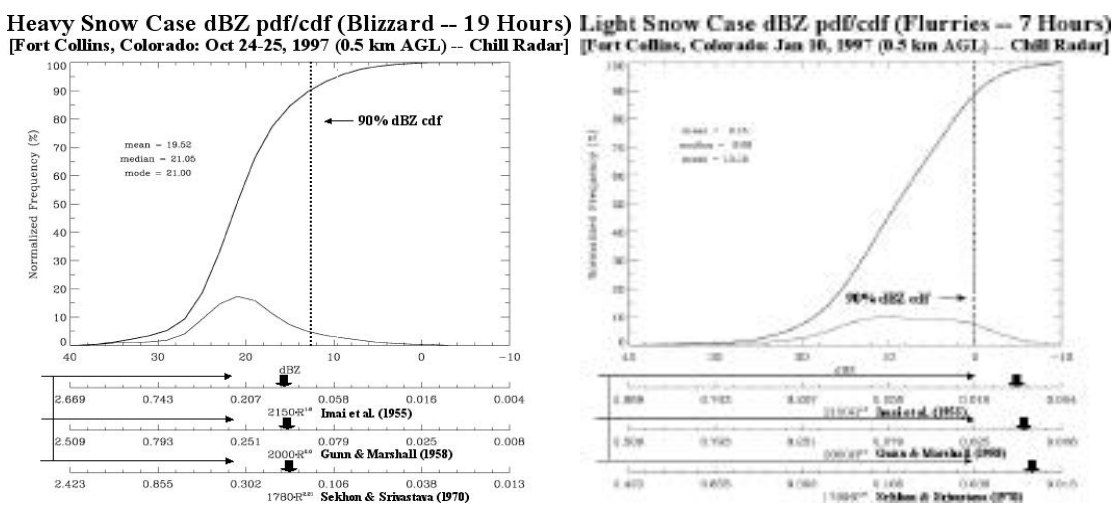

Figure 6b*:* Radar data analyses performed on Chill radar measurements obtained during heavy (left panel) and light (right panel) snowstorm cases from Fort Collins, CO -- indicating 90% CDF accumulation coordinates with respect to reflectivity factor axes (abscissas). Associated 90% snow water equivalent coordinates are shown below CDF diagrams according to three different Z-R relationships for snow. [Data provided courtesy of Prof. S. Rutledge, Colo. State Univ., Ft. Collins.]

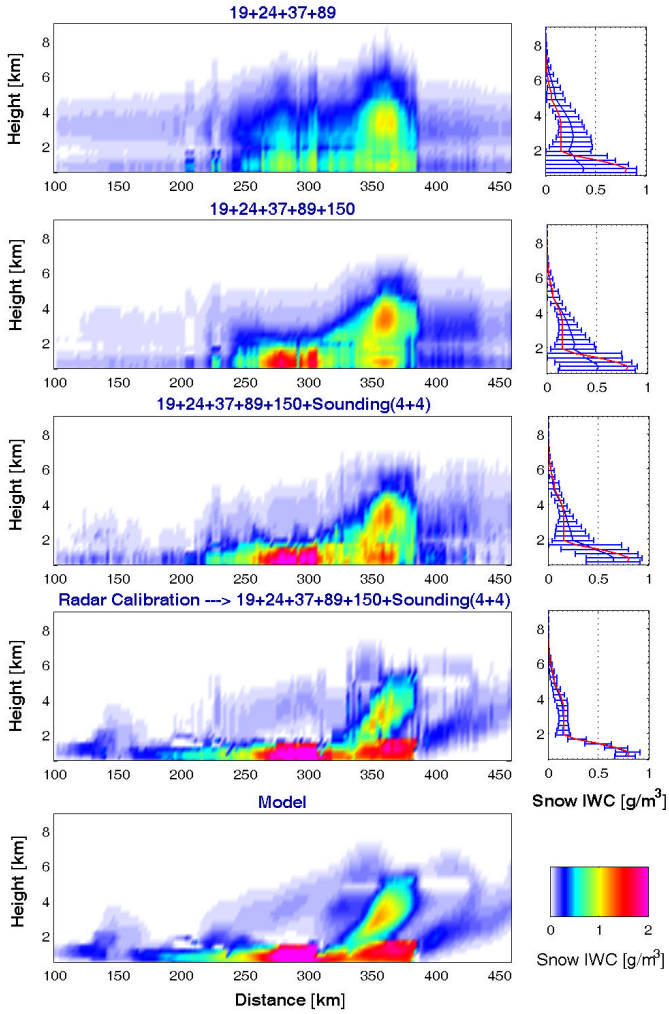

Figure 7: Synthetic snow IWC retrievals for selected cross-section of eastern U.S. snowstorm simulation. Left panels from top to bottom are: (1) EGPM radiometer retrieval using only four lower window frequencies, i.e. 18.7, 23.8, 36.5 and 89 GHz (similar to four SSM/I frequencies), (2) as previously but using all five window frequencies including 150 GHz, (3) as previously but using all five window frequencies plus four pairs of sounding channels in 50-54 and 118 GHz regions, (4) combined EGPM radar-radiometer retrievals, and for comparison (5) model "truth". For each retrieval case, associated right panels show estimated average profile (blue solid line) together with model "truth" average profile (red line), plus retrieval error standard deviations at various atmospheric levels (blue error bars).

These results can be summarized as follows:

- Retrievals based on the *four lower window frequencies* (i.e., SSM/I-like retrievals) do not provide an acceptable estimate of the snow profiles, but only gross differentiations among them. In particular, the heaviest profiles as well as snowfall just above the ground are greatly underestimated, while the structure of the lightest profiles is entirely missed (this being a consequence of a larger impact of surface emissivity on the observed T_Bs).

- *Addition of the highest window frequency at 150 GHz* largely improves the retrievals of the heaviest profiles and of snowfall just above the ground, by improving retrieval of the columnar snow contents. Nevertheless, there are cases (near 350 km) in which the snow profiles are incorrectly retrieved because the snow content is mainly associated with upper levels rather than just above the ground -- as with the model "truth". In addition, retrieval of the lightest profiles remains unsatisfactory.

- *Further addition of the sounding channels* significantly improves the retrievals, because of their small sensitivity to land surface emission compared to the window channels and because of their vertical profiling capability. In particular, retrieval of the shallow snow layer above the ground at 250-330 km is improved; the double-layer snow profiles near 350 km are better retrieved; and even the main characteristics of the lightest profiles are captured by the retrieval -- except the lack of precipitating snow above the ground between 400-450 km. Note that in this case, the average accuracy (bias and rms error) of near-ground snow profile retrievals is increased by a factor of 2.

- Finally, if the radiometer retrieval database is calibrated by vertical profile information obtained from radar observations, the *combined radar-radiometer* retrieval produces excellent results in every situation. Only in this case is a very low bias for the near-ground snow retrieval obtained. Also noteworthy is that a calibration of the radiometer database can be extended across the full swath of the radiometer.

Table 1: Average retrieval accuracy of near-ground (up to 500 m) snow IWC for four different retrievals shown in Fig. 5. Percentage values are calculated with respect to "truth" average value provided by UW-NMS model (0.784 g m^{-3}).

Configuration	**Bias** [g m^{-3}]	**rms error** [g m^{-3}]
Radiometer with channels at 18.7, 23.8, 36.5, and 89 GHz	-0.418 (-53%)	0.677 (86 %)
Radiometer with additional 150 GHz channel	-0.289 (-37%)	0.476 (61 %)
Radiometer with further additional (sounding) channels in 50-54 and 118 GHz regions	-0.145 (-18%)	0.301 (38 %)
Radar-calibrated EGPM radiometer	-0.026 (-3%)	0.104 (13 %)

6. CONCLUSIONS

A simulation study has been performed assessing the EGPM satellite's radar - radiometer sensitivity and retrieval performance for a meteorological relevant situation, i.e., a winter snowstorm. This type of precipitation event represents the primary observation target for the EGPM satellite. The main results of the investigation are summarized as follows:

- *Precipitating snow over land or snow cover* has distinct signatures at 89 and 150 GHz as well as at the paired sounding frequencies. The brightness temperature depressions due to scattering and the differential signatures at the 89-150 GHz frequencies and the 50 / 118 GHz frequency pairs contain detailed information on the presence of snow, on the vertical depth of the snow layer and concomitant cloud structure, on the snowfall rate, and on co-existing liquid precipitation.

- The *set of window frequencies* provides near-ground snow retrieval accuracies just meeting EGPM requirements in terms of rms error (50%), but exhibit too large a bias.

- The *sounding channels* are significantly less sensitive to surface emissivity variations than the window channels and provide significantly more information on snowfall and snow cover over land surfaces. As a consequence, these retrieval experiments show an increase in average accuracy (reduction in both bias and rms error) of near-ground snow profile retrievals by a factor of 2 when the sounding channels are used – an improvement that is sufficient to meet EGPM requirements.
- However, both the high frequency window channels and the sounding channels are necessary to optimize the snowfall retrievals.
- The high sensitivity (5 dBZ) EGPM *precipitation radar* will be able to observe the full vertical profile of precipitating snow, even in the case of light snowfall.
- The radiometric retrievals can be significantly improved if the radar measurements are used as a constraint for the radiometer inversions. Only in this case do the near-ground snow retrievals exhibit the preferred low bias.

These results demonstrate the potential of the full EGPM payload for snowfall measuring from space, and the enhancement to the International GPM mission made possible by EGPM participation in Earth Science's first international constellation partnership.

7. ACKNOWLEDGEMENTS

We wish to thank the EGPM Mission Advisory Group (MAG) of the European Space Agency (ESA) for all relevant discussions and inputs concerning the EGPM mission. [Besides five of the authors (A. Mugnai, P. Bauer, P. Joe, C. Kidd, and J. Testud), additional members of ESA's EGPM MAG are Dr. Paul Ingmann of ESA-ESTEC (Noordwijk, The Netherlands), Prof. Maria del Carmen Llasat of the University of Barcelona (Barcelona, Spain), and Prof. Giorgio Roth of the University of Genova (Genova, Italy).]. We also wish to thank Dr. Pedro Poiares Baptista of ESA-ESTEC, Dr. Ralf Bennartz of the University of Wisconsin (Madison, Wisconsin, USA), Dr. Vincenzo Levizzani of ISAC (Bologna, Italy), and Dr. Jim Weinman of the University of Washington (Seattle, Washington, USA) for useful discussions and insights regarding the snowfall retrieval problem. This study has been funded by ESA within the context of the EGPM supporting scientific studies carried out in the frame of Phase A, by the Italian National Group for Prevention from Hydro-Geological Disasters (GNDCI), by the Italian Space Agency (ASI), and within the frame of EURAINSAT – a shared-cost project (contract EVG1-2000-00030) co-funded by the Research DG of the European Commission (5th Framework Program).

8. REFERENCES

Bauer, P., L. Schanz, and L. Roberti, 1998: Correction of the three-dimensional effects for passive microwave remote sensing of convective clouds. *J. Appl. Meteor*., **37**, 1619-1632.

Bauer, P., and A. Mugnai, 2003: Precipitation profile retrieval using temperature-sounding microwave observations. *J. Geophys. Res*., **108**(D23), 4730-4743.

Blackwell, W.J., J.W. Barrett, F.W. Chen, R.V. Leslie, P.W. Rosenkranz, M.J. Schwartz, and D.H. Staelin, 2001: NPOESS Aircraft Sounder Testbed-microwave (NAST-M): Instrument description and initial flight results. *IEEE Trans. Geosci. Remote Sens.*, **39**, 2444-2453.

Bohren, C.F., and D.R. Huffman, 1983: *Absorption and Scattering of Light by Small Particles.* John Wiley & Sons, 530 pp.

da Silva, A.M., C.C. Young, and S. Levitus, 1994: *Atlas of Surface Marine Data 1994, Volume 1: Algorithms and Procedures.* NOAA Atlas NESDIS 6-8, U.S. Dept. of Commerce, NOAA, NESDIS, 83 pp.

Di Michele, S., F.S. Marzano, A. Mugnai, A. Tassa, and J.P.V. Poiares Baptista, 2003: Physically-based statistical integration of TRMM microwave measurements for precipitation profiling. *Radio Sci*., **38**, 8072-8088.

Di Michele, S., F.S. Marzano, A. Mugnai, A. Tassa, P. Bauer, and J.P.V. Poiares Baptista, 2004: The Bayesian algorithm for microwave-based precipitation retrieval (BAMPR): Description and application to TMI data. *IEEE Trans. Geosci Remote Sens.*, submitted.

Gasiewski, A.J., and D.H. Staelin, 1990: Numerical modeling of passive microwave O_2 observations over precipitation. *Radio Sci*., **25**, 217-235.

Grenfell, T.C., and S.G. Warren, 1999: Representation of a nonspherical ice particle by a collection of independent spheres for scattering and absorption of radiation. *J. Geophys. Res.*, **104**, 31697-31709.

Hewison, T., and S. English, 2000: Fast models for land surface emissivity. *Radiative Transfer Models for Microwave Radiometry* (C. Matzler, ed.), COST Action 712, Directorate-General for Research, European Commission, Brussels, Belgium, 117-127.

Heymsfield, A.J., and L.M. Miloshevich, 2003: Parameterizations for the cross-sectional area and extinction of cirrus and stratiform ice cloud particles. *J. Atmos. Sci*., **60**, 936-956.

Kongoli, C., P. Pellegrino, R.R. Ferraro, N.C. Grody, and H. Meng, 2003: A new snowfall detection algorithm over land using measurements from the Advanced Microwave Sounding Unit (AMSU). *Geophys. Res. Lett*., **30**, 1756-1759.

Kramer, H.J., 2002: *Observation of the Earth and its Environment: Survey of Missions and Sensors*. Springer-Verlag, 1510 pp.

Liebe, H.J., and G.G. Gimmestad, 1978: Calculation of clear air EHF refractivity. *Radio Sci*., **13**, 245-251.

Liebe, H.J., 1985: An updated model for millimeter wave propagation in moist air. *Radio Sci*., **20**, 1069-1089.

Liu, Q., C. Simmer, and E. Ruprecht, 1996: Three-dimensional radiative transfer effects of clouds in the microwave spectral range. *J. Geophys. Res*., **101**, 4289-4298.

Meneghini, R., and L. Liao, 2000: Effective dielectric constants of mixed-phase hydrometeors. *J. Atmos. Ocean. Tech*., **17**, 628-640.

Mugnai, A., S. Di Michele, F.S. Marzano, and A. Tassa, 2001: Cloud-model based Bayesian techniques for precipitation profile retrieval from TRMM microwave sensors. *Proc. ECMWF/EuroTRMM Workshop on Assimilation of Clouds and Precipitation*, ECMWF, Reading, U.K., 323-345.

Neshyba, S.P., T.C. Grenfell, and S.G. Warren, 2003: Representation of a nonspherical ice particle by a collection of independent spheres for scattering and absorption of radiation: 2. Hexagonal columns and plates. *J. Geophys. Res.*, **108**, 4448-4465.

Roberti, L., J. Haferman, and C. Kummerow, 1994: Microwave radiative transfer through horizontally inhomogeneous precipitating clouds. *J. Geophys. Res*., **99**, 16707-16718.

Skofronick-Jackson, G., M.-J. Kim, J.A. Weinman, and D.-E. Chang, 2004: A physical model to determine snowfall over land by microwave radiometry. *IEEE Trans. Geosci Remote Sens.*, in press.

Smith, E.A., A. Mugnai, K. Nakamura, R. Oki, J.M. Shepherd, and J. Testud, 2004: The Global Precipitation Measurement (GPM) concept. *Measuring Precipitation from Space: EURAINSAT and the Future*, Kluwer Publishers, this volume.

Tassa, A., S. Di Michele, A. Mugnai, FS. Marzano, and J.P.V. Poiares Baptista, 2003: Cloud-model based Bayesian technique for precipitation profile retrieval from TRMM Microwave Imager. *Radio Sci*., **38**, 8074-8086.

Tassa, A., S. Di Michele, A. Mugnai, F.S. Marzano, P. Bauer, and J.P.V. Poiares Baptista, 2004: Evaluation of cloud-radiation modeling errors for space-borne passive microwave retrieval of precipitation. *IEEE Trans. Geosci Remote Sens.*, submitted.

Tripoli, G.J., 1992: A nonhydrostatic model designed to simulate scale interaction. *Mon. Wea. Rev*., **120**, 1342-1359.

Wiscombe, W.J., 1980: Improved Mie scattering algorithms. *Appl. Opt*., **19**, 1505-1509.

Zwally, H.J., 1989: Growth of Greenland ice sheet: Interpretation. *Science*, **246**, 1589-1591.